Compact Objects and Binaries in Dense Star Clusters
Proceedings IAU Symposium No. 398, 2026
H. M. Lee, J. Hong & R. Spurzem, eds.
doi:10.1017/S1743921325104675

Tidal Tails and Their Dynamics in Open Clusters Using Gaia DR3

Ira Sharma[1,2], Vikrant Jadhav[3] and Annapurni Subramaniam[1]

[1]Indian Institute of Astrophysics, 2nd Block, Koramangala, Bangalore-560034, India
email: irasharma2208@gmail.com

[2]IISER Mohali, Knowledge City, Sector 81, SAS Nagar, Manauli PO 140306, Punjab, India

[3]Helmholtz-Institut für Strahlen- und Kernphysik, Universität Bonn, Nussallee 14-16, 53115 Bonn, Germany

Abstract. This research presents unsupervised machine learning and statistical techniques to detect and analyze tidal tails in five open clusters, BH 164, Alessi 2, NGC 2281, NGC 2354, and M67, with ages ranging from 60 Myr to 4 Gyr, using Gaia DR3 data. Color-magnitude diagram (CMD) matching, principal component analysis (PCA), and density-based clustering were used to detect the tails. Tidal tails were found in all clusters, extending 40 to 100 pc and containing 100 to 200 stars. Other statistical methods were used to study the stellar kinematics, photometry, and spatial distribution of the detected features. The tails had luminosity functions similar to their parent clusters, generally lacked massive stars, and showed higher binary fractions. Significant rotation was detected in M67 and NGC 2281 for the first time.

Keywords. Galaxy: kinematics and dynamics, open clusters and associations: general, methods: data analysis, astrometry, N-body simulations

1. Introduction

Tidal tails are extended stellar streams stretching from clusters due to the MW's gravitational effects, providing information about a cluster's dynamical state, trajectory, and mass loss history. Historically, the detection of open cluster tidal tails has been challenging due to low stellar densities and significant field star contamination from the Galactic disc. However, the Gaia mission, particularly Gaia DR2 (Gaia Collaboration 2018) and Gaia EDR3 (Gaia Collaboration 2021), with unprecedented astrometric accuracy, has greatly improved the detection of such extended features.

This study used Gaia DR3 (Gaia Collaboration 2023) to identify and examine tidal tails in five open clusters: BH 164, NGC 2354, Alessi 2, NGC 2281, and M67, chosen based on prior evidence of extended tidal structures (Bhattacharya *et al.* 2022; Tarricq *et al.* 2022; Hunt & Reffert 2023, 2024; Gao 2020b). The clusters span distances of 400–1300 pc and ages of 60 Myr–4 Gyr, which makes for a wide range of Galactic environments. We developed an optimized methodology to detect tidal tails in distant systems by combining clustering algorithms, kinematic analysis, and validation techniques, achieving significant improvements over earlier studies. The detailed research work is presented in Sharma *et al.* (2025).

2. Cluster Identification and Tidal Tail Detection

2.1. *Data Filtering and Preparation*

Proper motion (PM) cuts were applied using cluster-specific bounds based on the literature values of PM distributions. Stars with absolute PM errors < 0.5 mas/yr, positive

© The Author(s), 2026. Published by Cambridge University Press on behalf of The International Astronomical Union.

https://doi.org/10.1017/S1743921325104675 Published online by Cambridge University Press

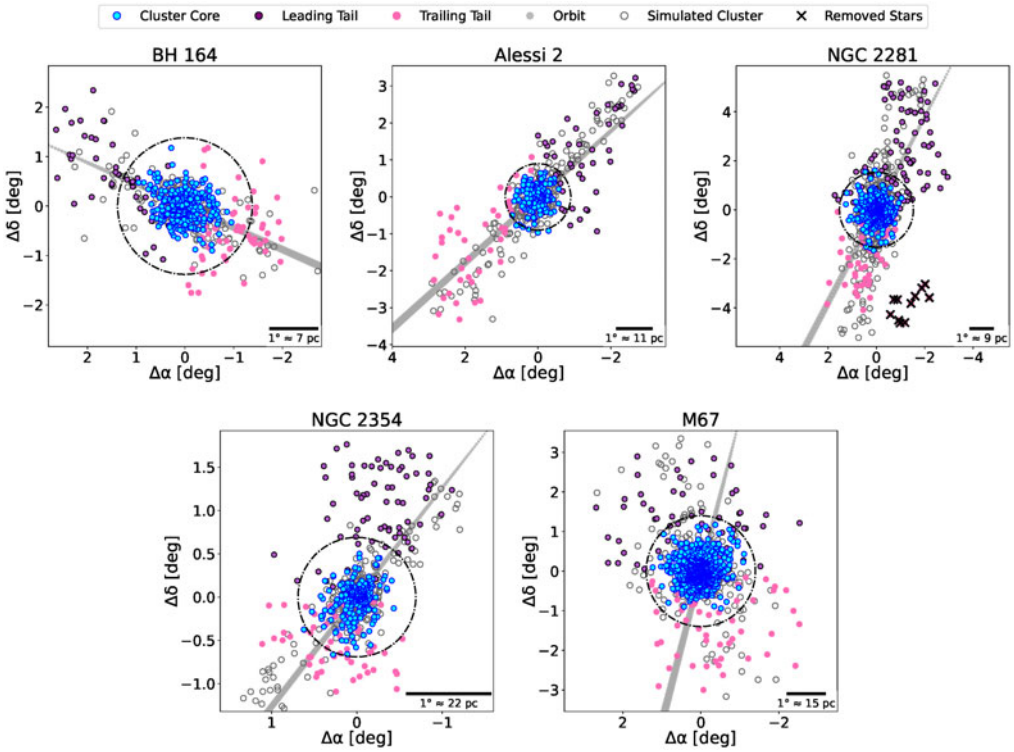


Figure 1. Spatial distribution of core members (blue dots), tidal tails (purple & pink dots), N-body simulated cluster (empty dots), Jacobi limit (dotted circle), and expected orbit (grey arrow) for the five clusters, with manually removed stars for NGC 2281 (crosses). For details, see Sharma *et al.* (2025).

parallaxes, and relative parallax errors $\sigma_{\varpi}/\varpi < 0.1$ formed the *Filtered Sample*. The identification of the core cluster used five normalized astrometric features: `ra`, `dec`, `pmra`, `pmdec`, and `distance`.

2.2. *DBSCAN Clustering*

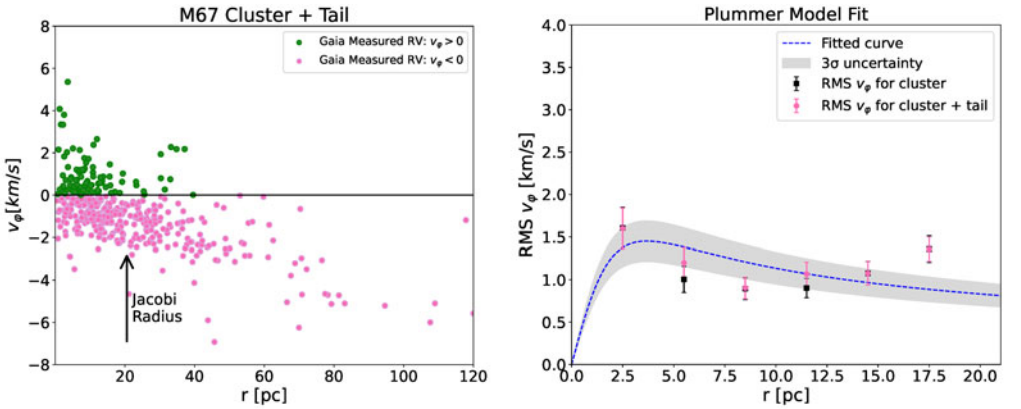
The DBSCAN (Density-Based Spatial Clustering of Applications with Noise) identifies groups of closely packed points while treating outliers as noise. The algorithm was run in the scaled 5D space to identify overdensities corresponding to the core cluster. Parameters (ϵ, min_neighbors) were tuned for high spatial completeness and low contamination.

2.3. *Tidal Tail Detection*

Following the core cluster identification, non-cluster members from the *Filtered Sample* within 500 pc of the mean cluster distance were tested for the tail membership using:

(1) **Radial Velocity (RV) Filtering**: A ±10 km/s window around the core cluster's mean radial velocity was applied only on the stars with available RV data as a loose filter to remove clear outliers while preserving plausible candidates.
(2) **CMD Matching**: KD-Tree structure helped in the efficient nearest-neighbor searches to identify stars with CMD properties similar to core members. A distance threshold of 0.05 in CMD space ensured photometric similarity, with the distance

https://doi.org/10.1017/S1743921325104675 Published online by Cambridge University Press



(a) Rotational velocity (v_φ) vs. distance from M67's center for cluster + tail stars.

(b) RMS v_φ vs. distance from M67's center with 3σ bounds and Plummer fit (core radius 2.6 pc).

Figure 2. Rotational analysis of M67 (See Section 3: item 5).

calculated as:

$$d_{\mathrm{CMD}} = \sqrt{(G - G_{\mathrm{core}})^2 + [(BP - RP) - (BP_{\mathrm{core}} - RP_{\mathrm{core}})]^2} \tag{1}$$

Only stars with $d_{\mathrm{CMD}} \leq 0.05$ were retained for further analysis.

(3) **Principal Component Analysis (PCA) and Clustering**: PCA was used to determine the cluster's primary elongation axis and align the coordinate frame accordingly. DBSCAN was then applied to the transformed spatial data to distinguish the tail stars from field noise.

(4) **Tangential Projection of the Celestial Coordinates**: Celestial coordinates were transformed to a 2D tangent plane using the cluster core's mean position as a reference to simplify the visualization and reduce spherical geometry effects.

(5) **Jacobi Radius Criterion**: The detected features were evaluated relative to the best-fit Jacobi radii (Hunt & Reffert 2024), beyond which the stars are prone to tidal stripping.

3. Tidal Tail Analysis

We examined the kinematics of the clusters and their tidal tails using proper motion corrections, orbital modelling, luminosity functions, binary statistics, and rotational dynamics.

(1) **Projection Effect Corrections**: Following van Leeuwen (2009), we fixed projection-induced distortions caused by bulk cluster motion and angular offsets in proper motions and radial velocities.

(2) **Orbit Integration**: Cluster orbits were computed with `Astropy` and `Galpy` using the `MWPotential2014` model, which made it possible to find the leading and trailing tail orientations in the orbital plane.

(3) **Luminosity Functions**: Using 1 mag bins in absolute magnitude (M_G), core cluster and tail luminosity functions were constructed. The relation $\log_{10} N \propto a \times M_G$ was used in linear fits, excluding the faintest bins because of observational incompleteness. The distributions of the core and tail stellar populations were compared using the Kolmogorov-Smirnov (KS) test.

(4) **Binary Fractions**: They were computed by identifying unresolved binaries in Gaia CMDs, using best-fitting PARSEC isochrones (Bressan *et al.* 2012) based on

https://doi.org/10.1017/S1743921325104675 Published online by Cambridge University Press

Table 1. Core cluster and tidal tail parameters for the five open clusters. Columns 1-3: Name and equatorial coordinates; Columns 4-5: Proper motions; Column 6: Mean RV of core cluster members; Column 7: Number of core members; Column 8: Number of tidal tail stars; Column 9: Best-fitting Jacobi radius from Hunt & Reffert (2024); Column 10: Total projected tip-to-tip extent of the tidal tails; Column 11-12: Binary fractions in the clusters and tails.

Name	RA (deg)	DEC (deg)	pmRA (mas/yr)	pmDEC (mas/yr)	RV (km/s)	N_{memb}	N_{tail}	r_J (pc)	L_{total} (pc)	$BF_{cluster}$	BF_{tail}
BH 164	222.20	−66.45	−7.41	−10.69	-3.4 ± 3.3	289	107	9.9	40	0.26 ± 0.04	0.26 ± 0.08
Alessi 2	71.61	55.16	−0.92	−1.08	-10.3 ± 4.2	130	100	9.6	90	0.22 ± 0.05	0.47 ± 0.12
NGC 2281	102.09	41.05	−2.96	−8.27	19.6 ± 4.6	438	136	13.6	91	0.24 ± 0.03	0.28 ± 0.08
NGC 2354	108.49	−25.73	−2.86	1.86	31.8 ± 5.5	244	142	14.9	69	0.34 ± 0.06	0.27 ± 0.08
M67	132.85	11.82	−10.97	−2.92	33.9 ± 3.4	1037	163	20.6	102	0.28 ± 0.02	0.30 ± 0.09

literature parameters. Main sequence ridge lines were estimated using ROBUSTGP (Li *et al.* 2020), with mass ratios calculated from main sequence shifts. Sources with mass ratios > 0.5 were classified as binaries.

(5) **Cluster Rotation**: Rotational properties were studied using the residual velocity method (Hao *et al.* 2022, 2024) to identify the rotation axes and compute the azimuthal velocity component v_φ. Analysis was limited to stars with reliable radial velocities ($G < 15$ mag, RV errors < 5 km/s), restricting the sample clusters to only M67 and NGC 2281. Radial profiles of v_φ and RMS v_φ were examined, with the Plummer model fitted for the mass estimation within the Jacobi radii for both clusters.

4. Results

All clusters exhibited tidal tails extending 1-4 times their Jacobi radii (Figure 2), with tail lengths of 40-100 pc. The youngest cluster (BH 164, 65 Myr) displayed the shortest tidal tail span, while the oldest (M67, 4 Gyr) exhibited the longest. Luminosity functions revealed a lack of high-mass stars in tails, and binary fractions were higher in tails, potentially due to dynamical interactions ejecting binaries. Rotation was found in the core and tails of M67 ($v_\varphi = -0.84 \pm 0.07$ km/s), while NGC 2281 showed rotation ($v_\varphi = -0.53 \pm 0.13$ km/s) mostly in its core. Both of them followed the Newtonian dynamics within their Jacobi radii. The Plummer model fits gave mass estimates of 832-876 $M_\odot$ for M67 and 741-803 $M_\odot$ for NGC 2281.

5. Conclusion

Our results showed that optimized clustering methods can detect extended structures up to a kiloparsec, increasing the range of clusters that can be studied compared to other techniques, such as the convergent point method, which is typically limited to within ≈400 pc. Moreover, detecting rotation in outer regions can also be used as a test for validating the presence of tidal tails, as 6D information is poor at larger distances. Extending this approach to more clusters can reveal hidden structures and refine dynamical models of cluster evolution.

Acknowledgements. I.S. acknowledges financial support from the International Astronomical Union through a travel grant to attend IAU Symposium 398 / MODEST-25. This work has made use of data from the European Space Agency (ESA) mission Gaia (https://www.cosmos.esa.int/gaia), processed by the Gaia Data Processing and Analysis Consortium (DPAC, https://www.cosmos.esa.int/web/gaia/dpac/consortium). AI-based tools were used for language editing purposes.

Supplementary material

To view supplementary material for this article, please visit https://doi.org/10.1017/S1743921325104675

https://doi.org/10.1017/S1743921325104675 Published online by Cambridge University Press

References

Bhattacharya, S., Rao, K. K., Agarwal, M., *et al.* 2022, *MNRAS*, 517, 3525
Bressan, A., Marigo, P., Girardi, L., *et al.* 2012, *MNRAS*, 427, 127
Gaia Collaboration, Brown, A. G. A., Vallenari, A., *et al.* 2018, *A&A*, 616, A1
Gaia Collaboration, Brown, A. G. A., Vallenari, A., *et al.* 2021, *A&A*, 649, A1
Gaia Collaboration, Vallenari, A., Brown, A. G. A., *et al.* 2023, *A&A*, 674, A1
Gao, X. 2020, *PASJ*, 72, 47
Hao, C. J., Xu, Y., Bian, S. B., *et al.* 2022, *ApJ*, 938, 100
Hao, C. J., Xu, Y., Hou, L. G., *et al.* 2024, *ApJ*, 963, 153
Hunt, E. L., & Reffert, S. 2023, *A&A*, 673, A114
Hunt, E. L., & Reffert, S. 2024, *A&A*, 686, A42
Li, L., Shao, Z., Li, Z.-Z., *et al.* 2020, *ApJ*, 901, 49
Sharma, I., Jadhav, V. V., Subramaniam, A., *et al.* 2025, arXiv:2508.19457
Tarricq, Y., Soubiran, C., Casamiquela, L., *et al.* 2022, *A&A*, 659, A59
van Leeuwen, F. 2009, *A&A*, 497, 209

https://doi.org/10.1017/S1743921325104675 Published online by Cambridge University Press